

Research Article

Phytochemical Profiling by HPLC-DAD, GC-MS, and ICP-OES and Bioactive Potential of *Salsola kali* L.: Structural Elucidation and ADME/T Evaluation for Pharmacological Insights

Haichour Rima ¹, Badis Aouzal ², Hamdi Bendif ³, Mehmet Öztürk ^{4,5},
Gulin Gumusbulut Sener ⁴, Fehmi Boufahja ³, Khellaf Rebbas ⁶, Elfalleh Walid ³,
Susana Rodríguez Couto ⁷ and Stefania Garzoli ⁸

¹Department of Ecology and Environment, Faculty of Natural and Life Sciences,

Natural Resources Valorization Laboratory (LVRN), Farhat Abbas Sétif-1 University, Sétif, Algeria

²Department of Nature and Life Sciences, Faculty of Sciences, University 20 August 1955, Skikda 21000, Algeria

³Biology Department, College of Science, Imam Mohammad Ibn Saud Islamic University (IMSIU), Riyadh 11623, Saudi Arabia

⁴Department of Chemistry, Faculty of Sciences, Muğla Sıtkı Koçman University, Muğla 48121, Türkiye

⁵Faculty of Chemistry and Chemical Technology, Al-Farabi Kazakh National University, Almaty, Kazakhstan

⁶Department of Natural and Life Sciences, Faculty of Sciences, University of M'sila, University Pole, Road Bordj Bou Arreiridj, M'sila 28000, Algeria

⁷Department of Separation Science, LUT School of Engineering Science, Lappeenranta-Lahti University of Technology LUT, Sammonkatu 12, Mikkeli 50130, Finland

⁸Department of Chemistry and Technologies of Drug, Sapienza University, Rome 00185, Italy

Correspondence should be addressed to Hamdi Bendif; hlbendif@imamu.edu.sa and Stefania Garzoli; stefania.garzoli@uniroma1.it

Received 20 March 2025; Revised 10 September 2025; Accepted 30 October 2025

Academic Editor: Munmun Bardhan

Copyright © 2025 Haichour Rima et al. Journal of Chemistry published by John Wiley & Sons Ltd. This is an open access article under the terms of the Creative Commons Attribution License, which permits use, distribution and reproduction in any medium, provided the original work is properly cited.

Salsola kali L., a halophytic plant renowned for its resilience in arid and saline environments, possesses a rich and diverse phytochemical profile with significant bioactive potential. This study provides a comprehensive phytochemical and pharmacological evaluation of *S. kali* extracts, employing an integrative analytical approach combining gas chromatography-mass spectrometry (GC-MS), inductively coupled plasma-optical emission spectrometry (ICP-OES), and high-performance liquid chromatography-diode array detection (HPLC-DAD). The phenolic composition of the methanolic extract revealed 17 identified compounds, with quercetin 3-O- β -galactoside (14.74 mg/g extract) and pyrocatechol (14.54 mg/g extract) being the most abundant, followed by other notable compounds highlighting the plant's phenolic diversity. Furthermore, bioavailability and pharmacokinetic properties of the identified bioactive compounds were predicted using SwissADME and pkCSM tools, revealing favorable drug-like characteristics. GC-FID analysis revealed that the hexane extract primarily contained saturated fatty acids, with palmitic acid being the most abundant, comprising 55.17% of total fatty acids. The mineral content analysis revealed a rich profile of essential macro- and micronutrients, with potassium (2.62%) as major constituents, alongside high levels of iron (379.82 mg/L). Pharmacological assessments demonstrated significant antioxidant activity, with the methanol extract showing moderate DPPH radical scavenging activity ($IC_{50} = 90.85 \pm 0.91 \mu\text{g/mL}$), while the hexane extract exhibited lower activity ($IC_{50} = 542.59 \pm 2.68 \mu\text{g/mL}$). The methanol extract also displayed promising enzyme inhibitory effects, with moderate activity against butyrylcholinesterase (BChE) and notable inhibition of α -glucosidase. However, acetylcholinesterase (AChE) inhibition was not observed at concentrations below 200 $\mu\text{g/mL}$. This study elucidates the structural and functional attributes of *S. kali* metabolites, emphasizing their potential as antioxidants, enzyme inhibitors, and nutrient sources for therapeutic use.

Keywords: antioxidant activity; bioavailability; enzyme inhibition; essential minerals; fatty acids; pharmacokinetics; phenolic compounds

1. Introduction

Plants represent valuable resources for medicinal exploration [1]. The genus *Salsola* (Amaranthaceae), previously classified under Chenopodiaceae, comprises over 140 species commonly found in arid and semiarid regions across the Middle East, Asia, Europe, and Africa [2, 3]. These species play significant roles in ecological restoration of saline soils [4]. Typically, *Salsola* species are shrubs or subshrubs with succulent, densely packed leaves adapted to harsh environments [5]. Despite its importance, most studies on the genus *Salsola* have focused on pollen morphology and species identification [6, 7], while fewer have explored its phytochemical composition and biological effects. Diverse phytoconstituents may be found in abundance within the *Salsola* genus, including flavonoids, phenolic compounds [8–10], fatty acids [11, 12], saponins, triterpenes, sterols, volatile constituents, lignans, coumarins, and cardiac glycosides, which contribute to its pharmacological properties, including analgesic, anti-inflammatory, antiviral, antibacterial, anticancer, cardioprotective, and hepatoprotective effects [13–17]. Plants from the genus *Salsola* hold significant importance in traditional medicine. For example, *Salsola somalensis* is valued for its hypotensive, antibacterial, and anticancer properties, with its dried roots being marketed as an anthelmintic in Ethiopia [15]. Additionally, the aqueous extracts of *Salsola tuberculatiformis*, which is a synonym for *Caroxylon tuberculiforme*, are also used by Bushmen women in Namibia and South Africa as an oral contraceptive device. According to Swartz et al. [18], this is accomplished by blocking the cytochrome P450-dependent 11 β -hydroxylase (P450c11) and decreasing the production of corticosteroids. *Salsola kali*, a facultative halophyte, is widely distributed across coastal areas, agricultural lands rich in seaweeds, and desert regions [19]. *S. kali* is also known as tumbleweed or Russian thistle [20]. Typically, this plant is found growing along roadsides, field edges, fallow areas, overgrazed pastures, and grasslands. It is an annual weed that thrives in arid locations and soils that are salty. The United States of America, Europe, North Africa, Asia, Australia, and Türkiye are among the countries that have a significant presence in its distribution [21]. Pharmacognostic analysis revealed its low moisture content, high ash values, and notable extractive and swelling indices, which are crucial for quality control and use in herbal medicine formulations [22]. Recently, bioactive compounds such as salsolanol, syringic acid, and tricin-7-O-glucopyranoside have been isolated from *S. kali*, emphasizing its medicinal value [23]. *Salsola kali* has a long history of use in traditional medicine for treating various health conditions, particularly cancer. According to El Bassossy et al. [23], it is considered to possess a wide variety of medicinal qualities, some of which include the following: diuretic, antihypertensive,

anticancer, purgative, emollient, antiulcer, and anti-inflammatory actions. Historically, the powdered whole plant has been utilized to alleviate coughs, while poultices made from chewed plant material have been applied to insect stings and employed in cancer treatment [24]. Furthermore, *S. kali* is noted for its potential in managing chronic conditions such as obesity, diabetes, and Alzheimer's disease, attributed to its antioxidant properties [25]. Beyond its medicinal uses, this plant also demonstrates significant environmental benefits, particularly in phytoremediation. It has shown a remarkable ability to extract cadmium from contaminated soils, underscoring its role in environmental cleanup efforts [26]. The valorization of bioactive compounds from agro-industrial waste has been also gaining attention due to their promising applications in health, food, and pharmaceutical industries [27].

Salsola kali is particularly renowned for its antioxidant properties, which arise from phenolic compounds produced in response to oxidative stress triggered by salinity, drought, and light intensity [28]. The plant's biological activities, including antioxidant, anti-inflammatory, and anticancer effects, are linked to its rich composition of alkaloids, flavonoids, phenolic acids, and other bioactive compounds [15, 16, 25, 29]. The biosynthesis and effectiveness of these compounds are influenced by various factors, such as the plant's genotype, developmental stage, and environmental conditions [30]. Collectively, *S. kali* and related species represent a valuable source of bioactive compounds, underscoring their importance in both medicinal and environmental applications. Given the limited data on the pharmacological potential and phytochemistry of Algerian *Salsola kali*, our research sought to investigate its chemical makeup and biological processes. Using high-performance liquid chromatography-diode array detection (HPLC-DAD), gas chromatography-mass spectrometry (GC-MS), and ICP-MS, we analyzed polyphenols, fatty acids, and mineral content in polar and apolar extracts. We also assessed antioxidant, anti-Alzheimer's, and antidiabetic properties. The findings offer new insights into its metabolic profile, nutritional value, and pharmacological potential, particularly its antioxidant and enzyme inhibitory effects. This study addresses key knowledge gaps through comprehensive phytochemical and pharmacological evaluations, demonstrating *S. kali*'s potential therapeutic applications due to its antioxidant and enzyme-inhibitory activities. Insights into bioavailability and mode of action provided here lay the groundwork for future medicinal and environmental studies.

2. Materials and Methods

2.1. Botanical Specimens. The stems and leaves of the *Salsola kali* plant (Figure 1) were collected in November 2023 in the M'sila region, situated in the northeast of Algeria (471 m



FIGURE 1: Photographs of the aerial parts of the plant *Salsola kali*, Msila, 2022 (photos: K. Rebbas).

above sea level (GPS coordinates: 35°42'20.99" N, 32°32'30.98" E) (Figure 1). Botanical determination was performed using Flora of Algeria (Quezel et Santa 1962–1963). Under the botanical collection number KR0052, the samples that were obtained were documented, and Professor K. Rebbas from the University of M'Sila in Algeria was the one who verified their identification. The identification was confirmed based on morphological characteristics and verified using the Plants of the World Online database [31–33]. After being washed with distilled water, the plant samples were dehydrated in an oven in the laboratory until they reached a weight that was consistent throughout. After the samples were dry, they were ground into a fine powder using an electric mill, and then they were sieved through a mesh size of 200 μm . For the duration of the subsequent analysis, the powdered samples were kept in a location that was cold, dry, and dark.

2.2. Preparation of Extracts. Forty grams of air-dried, powdered aerial parts of *S. kali* was extracted separately with methanol and hexane (200 mL each), through three sequential macerations (48–72 h at room temperature). Extracts were filtered (Whatman filter paper), evaporated under reduced pressure at 40°C, weighed, and stored at 4°C [34]. The method followed was adapted from Ertas et al. [35] and Aouzal et al. [36].

2.3. HPLC-DAD Analyses. In order to examine the phenolic compounds present in the methanol extract of *S. kali*, a Shimadzu HPLC system equipped with a DAD was employed [34]. This analysis was carried out in accordance with the methods described by Tokul-Ölmez et al. and published in 2020. The LC-solution program was utilized in order to carry out the investigation. The analysis was conducted using LC-solution software. Chromatographic separation was performed on an Inertsil ODS-3 column (4 μm , 4.0 mm \times 150 mm) at 40°C. An 8 mg/mL extract concentration in 80% methanol was prepared and filtered (0.45 μm), and 20 μL was injected. The mobile phase

comprised 0.1% acetic acid in water (A) and 0.1% acetic acid in methanol (B), with a 40-minute gradient elution. The flow rate was set at 1.5 mL/min, and phenolic compounds were detected at wavelengths of 230–350 nm, using UV data and retention times from 27 standards. Each analysis was conducted in triplicate, with results expressed as milligrams per gram of dry extract weight.

The technique's confirmation parameters, such as linearity range, limit of detection (LOD), limit of quantification (LOQ), and rehabilitation, were evaluated and computed following the approach outlined by Tokul-Ölmez et al. [37]. To ascertain the LOD and LOQ for each botanical compound analyte, standard solutions were systematically diluted and examined under the designated HPLC-DAD conditions until the minimal detectable concentration, aligned with a signal-to-noise (S/N) ratio of 3:1, was established. Subsequently, 10 replicate standard solution mixtures, incorporating internal standards, were formulated at the specified minimum detectable concentrations and introduced into the HPLC-DAD system. The LOD and LOQ values were later determined using the following equations:

$$\begin{aligned}\text{LOD} &= 3.3 \times \frac{\sigma}{\text{SS}}, \\ \text{LOQ} &= 10 \times \frac{\sigma}{\text{SS}}.\end{aligned}\tag{1}$$

According to Seal [38], the symbol σ is used to represent the standard deviation of the peak area, whereas the symbol SS is used to denote the slope of the calibration curve. The linearity of the approach was evaluated by creating calibration curves for each analyte across nine different concentration levels [34]. In order to guarantee that the results were reproducible, each concentration was examined in triplicate. Calibrating curves were generated by contrasting the ratio of the analyte concentration to the internal standard concentration (x-axis) with the corresponding ratio of the analyte peak area to the internal standard peak area (y-axis). This was done in order to analyze the relationship between the two variables. These curves were then used to determine the calibration of the instrument. The correlation

coefficients (R^2) were frequently above 0.99, which is proof that the approach demonstrated excellent linearity for all of the target substances within the concentration ranges that

were given. Application of the following formula to the data that were received allowed for the determination of the recovery:

$$\text{Recovery (\%)} = \frac{\text{Measured concentration} - \text{endemic concentration}}{\text{spiked concentration}} \times 100. \quad (2)$$

2.4. Physicochemical and Pharmacokinetic Properties for Computational Methods. The database SwissADME (<https://www.swissadme.ch/index.php>) is a state-of-the-art web resource providing free access to assess and predict essential molecular properties, including physicochemical attributes (e.g., molecular size/size, lipophilicity/LIPO, polarity/POLA, and insolubility/INSO), pharmacokinetics, druglikeness, and compatibility with medicinal chemistry for small molecules [39]. SIM F, ST-AMANT A, PAPAI I, SALAHUB DR. 1992. Gaussian density functional calculations on hydrogen-bonded systems. *J Am Chem Soc* 114: 4391–4400. Furthermore, it incorporates sophisticated instruments such as the BOILED-Egg model (forecasting gastrointestinal [GI] absorption and blood–brain barrier [BBB] permeability) and the Bioavailability Radar, which users can employ to enhance compound optimization strategies [39, 40].

pkCSM (available at <https://structure.bioc.cam.ac.uk/pkcsml>) is a crucial computational tool in pharmacological research. It integrates molecular properties such as physicochemical characteristics, pharmacophores, and toxicophores with distance-based graph signatures [41]. This approach enables medicinal chemists to systematically evaluate the relationships between pharmacokinetics, therapeutic efficacy, and toxicity, ultimately aiding in the design of safer and more effective drug candidates. Notably, features like the BOILED-Egg model and Bioavailability Radar enhance its predictive accuracy for druglikeness and bioavailability.

2.5. Analysis of Hexane Extract by GC-MS. 5 mg of the hexane extract was dissolved in 50 μL of anhydrous pyridine. Following this, 75 μL of bis(trimethylsilyl)trifluoroacetamide (BSTFA) was added and the mixture was incubated at 60°C for 20 min. After cooling, the solution was diluted with 375.0 μL of GC grade hexane, and 0.20 μL of the diluted silylated mixture was injected into the Varian 2100T GC-MS (Ion Trap, EI-mode, 70 eV) equipped with a Rtx-5 (30m \times 0.25 mm ID; 0.25 mm film thickness; crossbond 5% diphenyl + 95% dimethyl polysiloxane). Helium, with a pressure of 15 pounds per square inch and a purity of 99.999 percent, was used as the carrier gas, and the split ratio was 20 to 1. It was 280°C for the injection, 150°C for the ion trap, 180°C for the transfer line, and 120°C for the manifold. After adjusting the column temperature to 100°C for 5 min, it was raised to 300°C at a rate of 5°C/min, and then it was held at this temperature for 7 min. Finally, it was raised to 320°C at a rate of 20°C/min, and it was maintained for 7 min. The analysis time was 60 min. The mass range was adjusted

between m/z 28–650 amu. The NIST-Wiley 2014 library and the C_7 – C_{30} hydrocarbon mixture were used to elucidate the compounds [42]. Whenever possible, co-injections with those standards were used to elucidate the compounds.

2.6. Mineral Analyses. The procedure for the preparation of the sample was carried out in accordance with the protocol published by Cicero et al. [43] and Mokhtar et al. [34] with slight modifications.

Initially, the collected plant samples were cleaned, sliced, and oven-dried at 105°C for 24 h using a Nüve oven (Istanbul, Türkiye). After drying, the samples were homogenized with an IKA homogenizer (Staufen, Germany) and sieved through a 10-mesh screen, producing a uniform particle size of 1600 μm . The processed samples were stored in precleaned polyethylene bottles for further analysis. Deionized water with a resistivity of 18.2 $\text{M}\Omega\cdot\text{cm}^{-1}$ was prepared using a Milli-Q system (Human Power I Plus, Korea) and used for all aqueous solutions. Overnight, all of the glassware and plasticware was submerged in 10% nitric acid, and then it was completely cleaned with deionized water. This was done to prevent any contamination from occurring. In order to digest the plant material, 0.5 g of dry weight of the material was pulverized in a Teflon mortar and then digested with a CEM Mars 5 microwave closed system (CEM, Matthews, North Carolina, USA). Digestion was performed using an Ethos 1 microwave digester (Milestone, Bergamo, Italy) at 1000 W. Samples were treated with 6 mL of 65% nitric acid (HNO_3) and 2 mL of 30% hydrogen peroxide (H_2O_2), heated from 150°C to 200°C over 10 min, and held at 200°C for an additional 10 min. A twenty-minute ramp, a two-minute hold, and one hundred percent power at each step were the components of the program. Following digestion, the samples were allowed to cool to ambient temperature, filtered, and then diluted with ultra-pure water until they reached a final volume of one hundred milliliters. A blank digest was conducted in parallel with the produced solutions in order to detect any potential contamination. The solutions were stored at 4°C until they were analyzed. Using inductively coupled plasma-optical emission spectrometry (ICP-OES), which was carried out in accordance with the procedures described by Tel-Cayan et al. [44], the concentrations of minerals were determined. In order to guarantee the dependability of the findings, the precision of the analytical method was checked with the help of the standard reference material (SRM) NIST-CRM-1203 Drinking Water. The precision of the approach was demonstrated by the fact that the relative standard deviations (RSDs) constantly remained below 8% overall. All concentrations were stated

on a dry-weight basis, and the elemental analysis was carried out with the assistance of an Agilent 7700x ICP-MS technology. For the purpose of determining the likelihood of contamination, blank samples were included at every stage of the process, from the collecting of samples until the final analysis. The operational parameters for the ICP-MS instrument were as follows: RF power set at 1600 W, RF match at 2.10 V, sampling depth at 10.0 nm, nebulizer gas flow at 0.57 L/min, spray chamber with a Scott-type double-pass design, and argon flow rates of 15 L/min for plasma, 0.9 L/min for auxiliary, and 1.0–1.1 L/min for nebulizer, with a solution uptake rate of 1.8 mL/min. Giving the purpose of data collecting, peak hopping was utilized, and a replication time of 200 milliseconds, a dwell period of 200 milliseconds, and three readings were taken for each replicate, for a total of three samples.

2.7. Antioxidant Activity

2.7.1. Free Radical Scavenging Activity Using the DPPH Assay. Through the use of the DPPH assay, which was based on the technique proposed by Blois [45], the potential of *S. kali* extracts to scavenge free radicals was evaluated. The approach involved combining 40 μ L of plant extract at different concentrations with 160 μ L of a 1 mM DPPH solution in methanol onto a 96-well microplate. The quantities of the plant extract were varied. The combinations were allowed to sit in the dark at room temperature for a period of 30 min. The absorbance reading was taken with a microplate reader at a wavelength of 517 nm [46]. The blank was filled up with methanol. The following formula was utilized in order to determine the proportion of inhibition for every level at respective concentration:

$$\text{DPPH scavenging effect (\%)} = \left[\frac{(A_{\text{control}} - A_{\text{sample}})}{A_{\text{control}}} \right] \times 100. \quad (3)$$

A_{control} is the absorbance of the DPPH solution when it does not contain any extract, and A_{sample} is the absorbance when the extract is present in the solution.

The reduction in activity percentages was displayed across the extract levels, and the IC_{50} value, which indicates the concentration necessary to neutralize 50% of the DPPH radicals, was calculated. When comparing different antioxidants, BHT and BHA were utilized as reference antioxidants.

2.7.2. ABTS Cation Radical Decolorization Assay. To determine the level of antioxidant activity, the ABTS test that was developed by Re et al. [46, 47] was modified. The production of the ABTS cation radical solution was accomplished by allowing the reaction to take place in the dark at room temperature for a period of 12 hours. The process used 7 mM ABTS in water and 2.45 mM potassium persulfate. For the purpose of carrying out the experiment, a 96-well microplate was utilized to blend 40 μ L of plant extract (0.0625–4 mg/mL in methanol) with 160 μ L of ABTS

solution. At a wavelength of 734 nm, the absorbance was determined after a ten-minute incubation period in complete darkness. Methanol was the chemical in question. The percentages of inhibition were determined by using BHT and BHA as reference standards in the calculation.

2.7.3. Reducing Power Assay. After making some minor adjustments, the reduction capacity of *S. kali* extracts was assessed by using the method that was developed by Oyaizu [48]. For the experiment, the plant extracts were dissolved in methanol (10 μ L) and then combined with 40 μ L of phosphate buffer (pH 6.6) and 50 μ L of 1% potassium ferricyanide ($\text{K}_3\text{Fe}(\text{CN})_6$). The amounts of the plant extracts were controlled and varied. 20 min were spent incubating the mixture at a temperature of 50°C. This was followed by the addition of 50 μ L of 10% trichloroacetic acid, which was then followed by the addition of 40 μ L of distilled water and 10 μ L of 0.1% ferric chloride (FeCl_3). Measurements of absorbance were taken at a wavelength of 700 nm. Ascorbic acid was used as the reference standard to compare the reducing power agents [34].

2.7.4. Silver Nanoparticle (SNP) Reduction Assay. The silver ion (Ag^+) reduction technique, which was established by Ozyurek et al. [29], was also utilized in order to assess the antioxidant activity of *S. kali* preparations. In the reaction mixture, there were three components: 50 μ L of distilled water, 30 μ L of SNP power solution (1 mM AgNO_3 in a 1% citrate solution), and 20 μ L of plant extract produced in methanol at concentrations ranging from 0.0625 to 4 mg/mL. The absorbance was measured at 423 nm after 35 min of incubation at a temperature of 25°C. For the purpose of serving as reference antioxidants, ascorbic acid and Trolox worked.

2.8. Assays for the Inhibition of Enzymes. The enzyme inhibition potential of *S. kali* extracts was evaluated through in vitro spectrophotometric assays targeting acetylcholinesterase (AChE), butyrylcholinesterase (BChE), α -amylase, and α -glucosidase. The assays were performed using a 96-well microplate reader (SpectraMax³⁴⁰PC384, Molecular Devices, Silicon Valley, CA, USA), with data processing handled via SoftMax Pro v5.2 software. All tests were conducted using appropriate controls to ensure reliability, and the IC_{50} values, representing the concentration required for 50% inhibition, were calculated for each enzyme.

2.8.1. Anticholinesterase Activity. The inhibitory effects on AChE and BChE were assessed following the protocols by Ellman et al. [49] and Topal [11]. Stock solutions of the extracts were prepared at a concentration of 2000 μ g/mL. The assay measured the hydrolysis of acetylthiocholine into thiocholine, which reacts with 5,5'-dithiobisnitrobenzoate (DTNB) to produce a yellow 5-thio-2-nitrobenzoate anion. The reaction setup included 20 μ L of AChE (5.32×10^{-3} U) or BChE (6.85×10^{-3} U) enzyme, 150 μ L of sodium

phosphate buffer (0.1 M, pH 8.0), and 10 μ L of extract at varying concentrations, incubated at 25°C for 15 min. The reaction was initiated by adding 10 μ L of acetylthiocholine iodide (7.1×10^{-4} M) or butyrylcholine chloride (2×10^{-4} M)

and 10 μ L of DTNB (5×10^{-4} M). Absorbance at 412 nm was recorded every 5 min for 15 min. Galanthamine served as a reference standard. The inhibition percentage was calculated using the formula:

$$\text{Inhibition} = \left[\frac{(\text{Enzyme activity without extract} - \text{Enzyme activity with extract})}{\text{Enzyme activity without extract}} \right] \times 100. \quad (4)$$

2.8.2. α -Amylase Inhibitory Activity. In order to conduct the α -amylase inhibition experiment, adjustments were made to the methodology described by Van Quan et al. [50]. The extract solution, which had between 50 and 400 μ g/mL, was combined with 50 μ L of α -amylase solution, which contained 0.1 units/mL, in a 96-well plate. The phosphate buffer, which had a pH of 6.9 and contained 6 mM sodium chloride, was 20 mM. A mixture was preincubated at 37°C for 10 min, and then 50 μ L of a starch solution containing 0.05% was added. This was followed by another 10 min of incubation at 37°C. In order to bring an end to the process, 25 μ L of 0.1 M hydrochloric acid and 100 μ L of Lugol solution were introduced. A measurement of absorbance was taken at 565 nm. Since acarbose was the reference standard, it was implemented.

2.8.3. α -Glucosidase Inhibitory Activity. For the α -glucosidase inhibition experiment, Kim et al. [51] served

as the source of inspiration. In a plate with 96 wells, the reaction mixture consisted of 50 μ L of phosphate buffer with a pH of 6.9, 25 μ L of 4-N-nitrophenyl- α -D-glucopyranoside (PNPG) in phosphate buffer, 10 μ L of extract solution containing 25–200 μ g/mL, and 25 μ L of α -glucosidase solution with 0.1 units per milliliter in 0.01 M phosphate buffer with a pH of 6.0. In order to halt the reaction, the mixture was subjected to incubation at 37°C for a duration of 20 min. Subsequently, 90 μ L of 0.1 M sodium carbonate was added to the mixture. A measurement of absorbance was taken at 400 nm. Acarbose was used as a benchmark for further comparison. Graphical analysis was performed to obtain the IC₅₀ values for α -amylase and α -glucosidase inhibition. This was accomplished by plotting the percentage of inhibition against the log-transformed quantity of sample concentrations. The following formula was utilized in order to ascertain the percentages of inhibition:

$$\text{Inhibition (\%)} = \left[\frac{(\text{Absorbance of control} - \text{Absorbance of the test})}{\text{Absorbance of control}} \right] \times 100. \quad (5)$$

2.9. Statistical Analysis. All biological assessment results are presented as the mean \pm standard error of the mean (SEM) of three independent replicates. Tukey's honest significant difference (HSD) test was utilized in situations where the p value was less than 0.05. This test was utilized to assess whether or not there were significant differences between the means of the extracts and the standards by means of multiple comparisons. For all statistical tests, results were deemed significant at a threshold of $p < 0.05$.

3. Results and Discussion

3.1. HPLC-DAD Analyses. HPLC-DAD analysis identified 17 phenolic compounds in *S. kali* methanol extract (Table 1 and Figure 2). The predominant compounds included quercetin 3-O- β -galactoside (14.74 mg/g), pyrocatechol (14.54 mg/g), quercetin 3-O-neohesperidin (11.23 mg/g), and luteolin 7-O- β -glucoside (10.44 mg/g). Other compounds appeared at lower concentrations (0.24–9.09 mg/g), confirming the plant's diverse phenolic profile [52]. This study represents the first investigation into the phenolic composition of *S. kali* methanolic extract from Algeria, aligning with earlier reports of simple phenols such as

catechol and resorcinol in this species [10, 14]. The observed phenolic diversity underscores *S. kali*'s unique metabolic profile, characterized by high levels of quercetin 3-O- β -galactoside (14.74 mg/g extract), pyrocatechol (14.54 mg/g extract), quercetin 3-O- β -neohesperidin (11.23 mg/g extract), quercetin 3-O- β -glucoside (10.44 mg/g extract), epicatechin (9.09 mg/g extract), rutin (9.07 mg/g extract), and fumaric acid (8.66 mg/g extract), which collectively distinguish it from other species within the *Salsola* genus (Table 1). Notably, pyrocatechol, the predominant phenolic compound, has not been reported in such high concentrations in other *Salsola* species, highlighting *S. kali*'s distinct metabolic traits. In addition to its flavonoid diversity including flavone glycosides (e.g., luteolin-7-O- β -D-glucoside), flavonols (e.g., quercetin), and flavanols (e.g., epicatechin), *S. kali* exhibits a unique phenolic composition. Other species such as *S. imbricata*, *S. vermiculata*, and *S. collina* share common phenolic acids like gallic, caffeic, ferulic, and chlorogenic acids [53, 54]. *S. kali* stands out due to its elevated levels of pyrocatechol and flavone glucosides, alongside good concentrations of caffeoylquinic acid (e.g., caffeic and ferulic acids). This suggests a distinct metabolic pathway in *S. kali*, differentiating it from its congeners. Furthermore, the

presence of fumaric acid, known for its antioxidant and anti-inflammatory properties [34], enhances *S. kali*'s metabolic profile and underscores its potential bioactivity. Comparative studies with species like *S. vermiculata*, *S. tetrandra*, and *S. collina* [53, 54] reveal shared phenolic acids but confirm *S. kali*'s uniqueness due to its high rutin, pyrocatechol, and epicatechin content. Similar findings regarding the potential of phenolic-rich extracts from agricultural by-products have been recently reported by Neagu et al. [27], highlighting the growing interest in agro-industrial residues as valuable sources of bioactive compounds [36].

The unique phenolic composition of *S. kali* likely reflects species-specific metabolic adaptations to environmental stressors, supporting its therapeutic potential. This distinct chemical profile underscores the importance of further exploring its pharmacological applications [46, 55, 56].

3.2. Druglikeness Properties. SwissADME is a widely used database in the early stages of drug discovery, design, and development. It enables the prediction of key physicochemical and pharmacokinetic properties of compounds. Table 2 provides a detailed analysis of the physicochemical properties, lipophilicity, druglikeness, bioavailability, and pharmacokinetics of various compounds identified in *Salsola kali*. The bioavailability scores (BASs) for these compounds ranged from 0.11 to 0.85, indicating acceptable bioavailability for all components.

Lipinski's rule of five, a widely accepted guideline for predicting drug-like properties, was applied to assess the potential for oral bioavailability [57]. Experimental and computational approaches to estimate solubility and permeability in drug discovery and development settings. Adv Drug Deliv Rev 46: 3–26. According to this rule, a compound is more likely to be orally bioavailable if it meets the following criteria: molecular weight ≤ 500 g/mol, $\log p \leq 5$, ≤ 10 hydrogen bond acceptors (n-ON), and ≤ 5 hydrogen bond donors (n-OHNH) [58]. Compounds 1–7, 11, 15, 16, and 17 follow Lipinski's rule, suggesting they are more likely to be orally bioavailable. Compounds 8, 9, 10, 12, 13, and 14 violate the rule, indicating potential challenges in oral bioavailability. Additionally, the $\log p$ values for all compounds were below 5, further supporting their drug-like properties.

All compounds demonstrated high GI absorption, except luteolin 7-O-rutinoside, rutin, quercetin 3-O-neohesperidin, luteolin 7-O- β -glucoside, quercetin 3-O- β -galactoside, and 3,5-O-dicaffeoylquinic acid which were identified as BBB permeants due to their lower GI absorption. The topological polar surface area (TPSA), a key parameter influencing membrane permeability, is generally considered favorable for oral bioavailability when $< 70 \text{ \AA}^2$. In this study, only three compounds: pyrocatechol, methyl-1,4-benzoquinone, and ferulic acid exhibited TPSA values below this threshold. However, it is important to note that TPSA values above 70 \AA^2 do not necessarily preclude bioavailability, as other factors such as molecular flexibility and polarity also play significant roles.

Skin permeability, expressed as $\log K_p$, measures the compound's ability to permeate the skin. In this report, it ranged between -10.26 and -5.80 cm/s, with more negative values indicating lower permeability; in addition, compounds with higher $\log K_p$ values (e.g., 17) are more likely to be absorbed through the skin [59].

Regarding synthetic accessibility scores, the compounds varied from 1.00 to 6.52, suggesting that they are relatively easy to synthesize [60–62]. The molar masses of the compounds ranged from 110.11 g/mol to 610.52 g/mol; compounds with molecular weights below 500 g/mol are generally considered more drug-like which are aligning with Lipinski's recommendation for optimal bioavailability.

Among the phenolic compounds identified in *S. kali*, 1–7, 11, 15, 16, and 17 were determined to adhere to rule five of Lipinski. These compounds were predicted to exhibit good oral bioavailability due to their favorable physicochemical properties, including small molecular size, appropriate polarity, and flexibility, which enhance their permeability across biological membranes, particularly in the GI tract. Their solubility in aqueous environments further supports their potential as oral bioavailable drug candidates [63].

This detailed analysis can guide further research into the therapeutic potential of *Salsola kali* compounds, focusing on those with favorable drug-like properties and pharmacokinetic profiles.

3.3. Chemical Structure and Bioavailability Radar. The Bioavailability Radar (Figure 3) is defined by two-dimensional structural pictures generated via the JChem website (<https://chemaxon.com/jchem>) in conjunction with canonical SMILES notations sourced of PubChem (<https://pubchem.ncbi.nlm.nih.gov>), with each component presented on a separate line in the output. Furthermore, the radar defines six important physicochemical properties: lipophilicity, size, polarity, solubility, flexibility, and insaturation. A physicochemical range appeared as a pink area, and molecules plotted entirely within it are considered drug-like.

3.4. "BOILED-Egg" Model. A graphical tool is the BOILED-Egg model (Figure 4), which can be found in SwissADME used to predict BBB and the GI absorption penetration (HIA) of chemical compounds. By mapping compounds based on their physicochemical properties, it classifies them into either the white zone (high GI absorption) or the yellow zone (potential brain penetration). This visualization aids in assessing pharmacokinetic properties, thereby supporting decision making in drug development and optimization [39]. Furthermore, it consists of a white region, which illustrates the physicochemical area for the extremely intake of HIA that predicted that all the 17 identified compounds possess high GI absorption. On the other hand, the yellow region (yolk) symbolizes the physicochemical space for highly probable BBB permeation. In our study, based on

TABLE 1: Phenolic composition of the extracts of *Salsola kali* by HPLC-DAD (mg/g dry extract).

Peak	Compounds	RT ^a	Calibration equation	R ^{2b}	Linear range (µg/mL)	λ _{max} nm	LOD ^c (µg/mL)	LOQ ^c (µg/mL)	Recovery	RSD ^d within day (n: 7)	S. kali (mg/g)
1	Fumaric acid	13.3	y = 1988.9x - 4655.8	0.9998	7.5-125	254	1.29	3.98	102.45 ± 6.96	4.96	8.66
2	Pyrocatechol	23.1	y = 3772.8x + 23,692	0.9925	11.3-500	254	4.78	14.48	103.07 ± 5.46	5.44	14.54
3	Theobromine	25.9	y = 3942.7x + 81,451	0.9983	15-85	254	10.11	30.13	95.11 ± 5.42	6.53	tr
4	Catechin	29.9	y = 2611.2x + 74,392	0.9972	7.6-500	254	3.29	9.96	102.11 ± 4.08	3.78	1.08
5	Methyl- <i>p</i> -benzoquinone	33.7	y = 370,60x - 637,474	0.9934	6.13-50.0	254	5.37	16.27	103.03 ± 4.23	4.86	2.87
6	Caffeic acid	35.3	y = 495,33x + 213,471	0.9957	5.01-30.0	254	4.54	13.75	102.67 ± 4.92	4.01	0.24
7	Epicatechin	35.7	y = 2097.6x + 7998.2	0.998	1.9-500	254	0.95	2.86	101.25 ± 1.85	4.00	9.09
8	Luteolin 7-O-rutinoside	40.5	y = 478,99x + 56,096	0.9997	2.00-45	254	1.15	3.45	99.92 ± 2.11	4.15	0.73
9	Rutin	41.2	y = 451,52x + 52,145	0.9997	3.13-200	254	2.49	7.56	101.99 ± 3.45	3.01	9.07
10	Quercetin 3-O-neohesperidin	41.8	y = 351,45x + 34,062	0.9997	1.56-50	254	1.00	3.30	100.92 ± 3.65	5.16	11.23
11	Ferulic acid	42.5	y = 422,45x + 110,701	0.9992	4.34-300	254	3.96	11.99	100.99 ± 3.54	3.20	0.75
12	Luteolin 7-O-β-glucoside	43.3	y = 395,22x + 45,156	0.9997	2.00-100	254	1.00	3.30	104.11 ± 3.81	4.22	10.44
13	Quercetin 3-O-β-galactoside	45.7	y = 478,99x + 56,096	0.9997	3.13-100	254	1.00	3.30	98.42 ± 4.74	4.86	14.74
14	3,5-O-Dicaffeoylquinic acid	50.3	y = 425,59x - 2,000,000	0.9959	4.00-128	254	2.50	8.25	97.63 ± 5.01	3.12	7.93
15	Fisetin	51.1	y = 10,078.4x + 16,688	0.9984	1.56-100	254	1.01	3.06	98.57 ± 3.84	1.87	7.20
16	Luteolin	58.8	y = 895,69x - 62,198	0.9995	4.84-620	254	2.75	8.34	100.00 ± 4.91	2.88	0.75
17	Apigenin	63.9	y = 719,90x + 62,472	0.9996	0.66-170	254	0.65	1.96	98.80 ± 5.01	1.36	0.30

^aRT: retention time of the compound in minutes.^bR²: the linearity of the calibration graph.^cLOD: limit of detection in µg/mL and LOQ: limit of quantification in µg/mL.^dRSD: percentage relative standard deviation; tr: trace amounts.

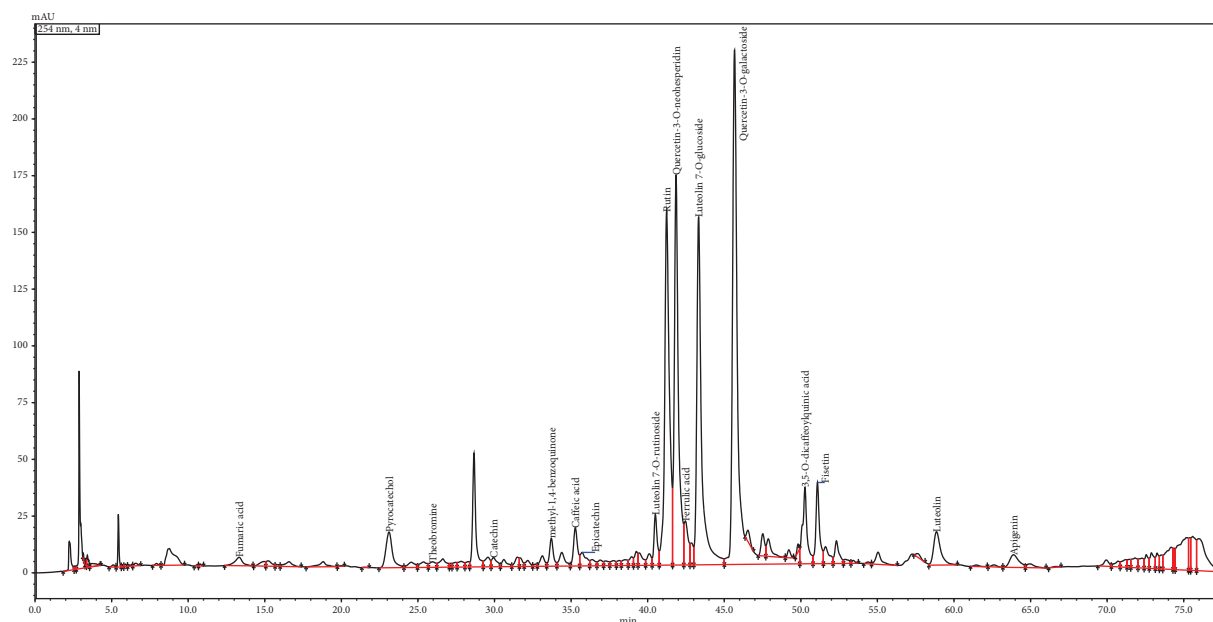


FIGURE 2: HPLC-DAD chromatogram of *Salsola kali* at 254 nm.

their physicochemical properties, pyrocatechol (2), methyl-1,4-benzoquinone (5), and ferulic acid (11) were hypothesized to be capable of breaking through the BBB. The compounds falling outside the egg are accounted to have less absorption and lower penetration to the BBB than luteolin 7-O- β -glucoside (12).

The column of AMES toxicity indicates whether the compound is mutagenic (i.e., can cause mutations in the DNA) based on the Ames test. A “Yes” means the compound is mutagenic, while a “No” means that is not mutagenic. According to the data in Table 3, only theobromine showed a “Yes,” which means that the compound is mutagenic. The column of Max. tolerated dose (human) demonstrates the maximum dose of a molecule that can be tolerated by humans, expressed in log mg/kg/day. Thus, the high value of 1.145 obtained for caffeic acid indicated that it can be tolerated at higher doses than pyrocatechol which presented a negative value (−0.017). In addition, the column of oral rat acute toxicity (LD_{50}) exhibits the lethal dose (LD_{50}) for rats when the substance is administered orally expressed in mol/kg.

Lower LD_{50} values indicate higher acute toxicity. For example, fumaric acid (LD_{50} = 1.626 mol/kg) shows greater toxicity than theobromine (LD_{50} = 2.385 mol/kg).

Furthermore, the column of hepatotoxicity indicates whether the component has the potential to cause liver damage. A “Yes” means the compound is hepatotoxic; however, a “No” means it is not hepatotoxic. The obtained results (Table 3) denoted that only pyrocatechol and luteolin 7-O-rutinoside show hepatotoxic potential.

The compounds identified in *Salsola kali* generally possess low toxicity profiles, with exceptions (e.g., pyrocatechol and theobromine). Furthermore, most molecules are nonmutagenic and nonhepatotoxic, making them potentially safe for further pharmacological or nutritional studies. However, compounds such as

pyrocatechol and theobromine should be used with caution due to their mutagenic and hepatotoxic potential. As conclusion, the analysis data suggest that *Salsola kali* possesses several bioactive compounds with favorable ADME properties, which could be explored for therapeutic applications.

3.5. Fatty Acid Analysis by GC-FID. The fatty acid composition of *S. kali* hexane extract, determined by GC-FID, highlighted the presence of various saturated and unsaturated fatty acids, along with long-chain hydrocarbons. The *S. kali* hexane extract has a fatty acid profile that was dominated by saturated fatty acids, with palmitic acid being the most abundant fatty acid, accounting for 55.17% of the total contents. Hydroxylated derivatives like 3-hydroxypalmitic acid and hydrocarbons like pentacosane, heptacosane, and nonacosane were present in less amounts (Table 4).

Saturated fatty acids and hydrocarbons make up the majority of the lipid profile that was discovered through the use of GC-FID to analyze the fatty acid content of the *Salsola kali* hexane extract (Table 5). The GC-FID chromatogram is reported in Figure 5. Among the detected compounds, palmitic acid was the most abundant, accounting for 55.17% of the total fatty acid content. Additional saturated fatty acids, including tetradecanoic acid, heptadecanoic acid, and stearic acid, were also detected in minimal quantities. This profile aligns with typical plant-based extracts, where saturated fatty acids contribute significantly to structural and metabolic functions. Hydroxylated derivatives, particularly 3-hydroxypalmitic acid, and hydrocarbons like pentacosane, heptacosane, and nonacosane were also identified in minor concentrations. In spite of the fact that they are not very abundant, these chemicals are well known for the bioactive qualities

TABLE 2: Forecasting of physicochemical attributes, bioavailability, druglikeness, lipophilicity, and pharmacokinetics with SwissADME.

	1	2	3	4	5	6	7	8	9	10	11	12	13	14	15	16	17
The <i>Salsola kali</i> identified																	
<i>Physicochemical properties/lipophilicity</i>																	
Molecular weight	116.07	110.11	110.11	180.16	180.16	290.27	178.14	122.12	290.27	180.16	152.15	448.38	464.38	516.45	286.24	286.24	270.24
No. Heavy atoms	8	8	8	13	13	21	13	9	21	13	11	32	33	37	21	21	20
iNo. arom	0	6	6	9	9	12	10	0	12	6	6	16	16	12	16	16	16
Fraction Csp ³	0.00	0.00	0.00	0.29	0.29	0.20	0.00	0.14	0.20	0.00	0.12	0.29	0.29	0.24	0.00	0.00	0.00
No. rotatable bonds	2	0	0	0	0	1	0	0	1	2	2	4	4	9	1	1	1
No. H-bond acceptors	4	2	2	3	3	6	4	2	6	4	3	11	12	12	6	6	5
No. H-bond donors	2	2	2	1	1	5	2	0	5	3	1	7	8	7	4	4	3
Molar refractivity	24.41	30.49	30.49	47.14	47.14	74.33	46.53	33.10	74.33	47.16	40.34	108.13	110.16	126.90	76.01	76.01	73.99
TPSA (Å ²)	74.60	40.46	40.46	72.68	72.68	110.38	70.67	34.14	110.38	77.76	46.53	190.28	210.51	211.28	111.13	111.13	90.90
Consensus log po/w	-0.35	0.97	0.97	-0.12	-0.19	0.83	1.12	0.82	0.85	0.93	1.20	0.15	-0.38	0.79	1.55	1.73	2.11
<i>Druglikeness, bioavailability, pharmacokinetics</i>																	
Lipinski's rule	Yes	Yes	Yes	Yes	Yes	Yes	Yes	Yes	Yes	Yes	Yes	No	No	No	Yes	Yes	Yes
Bioavailability score	0.85	0.55	0.55	0.55	0.55	0.55	0.55	0.55	0.55	0.56	0.55	0.17	0.17	0.55	0.55	0.55	0.55
GI absorption	High	High	High	High	High	High	High	High	High	High	High	Low	Low	Low	High	High	High
BBB permeant	No	No	No	No	No	No	No	Yes	No	No	Yes	No	No	No	No	No	No
P-gp substrate	No	No	No	No	No	Yes	No	No	Yes	No	No	Yes	No	Yes	No	No	No
CYP1A2 inhibitor	No	No	No	Yes	No	No	Yes	No	No	No	No	No	No	No	Yes	Yes	Yes
CYP2C19 inhibitor	No	No	No	No	No	No	No	No	No	No	No	No	No	No	No	No	No
CYP2C9 inhibitor	No	No	No	No	No	No	No	No	No	No	No	No	No	No	No	No	No
CYP2D6 inhibitor	No	No	No	No	No	No	No	No	No	No	No	No	No	No	Yes	Yes	Yes
CYP3A4 inhibitor	No	No	No	No	No	No	No	No	No	No	No	No	No	No	Yes	Yes	Yes
Log Kp (cm/s)	-7.25	-6.35	-6.35	-7.82	-7.95	-7.82	-6.52	-6.53	-7.82	-6.58	-6.37	-8	-8.88	-8.37	-6.65	-6.25	-5.80
Synthetic accessibility	1.80	1.00	1.00	1.93	1.87	3.50	2.61	2.69	3.50	1.81	1.15	5.17	5.32	4.81	3.16	3.02	2.96

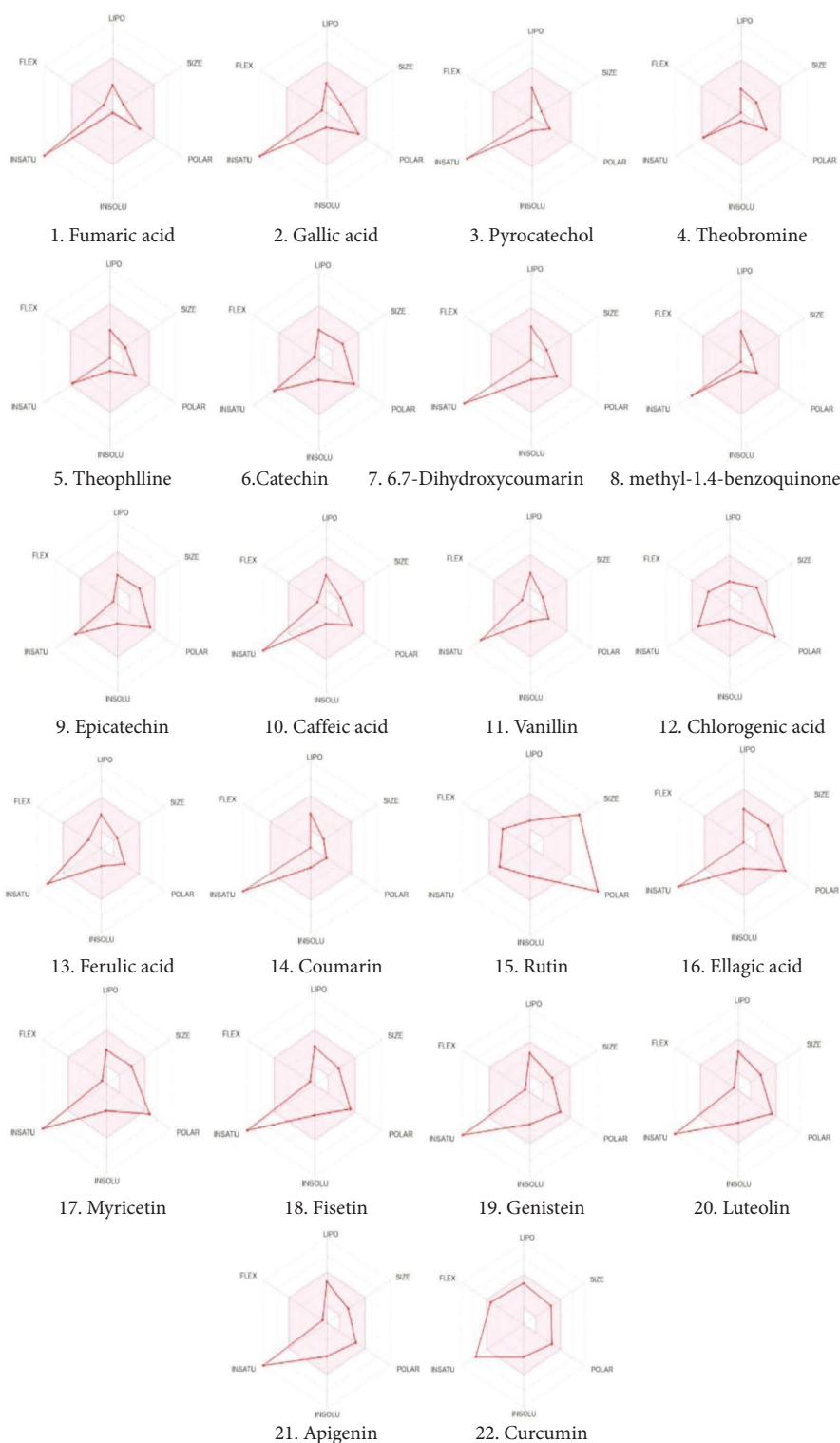


FIGURE 3: Bioavailability hexagons of the major molecules identified in *Salsola kali* determined by HPLC-DAD analysis: Lipophilicity; molecular size; polarity; insolubility; insaturation; flexibility.

that they possess and have the potential to contribute to the organism's total biological activity. However, their minimal concentrations suggest a limited role compared to the more abundant saturated fatty acids. In contrast to these findings, previous studies have highlighted the prevalence

of unsaturated fatty acids in other *Salsola* species. For instance, Rasheed et al. [15] reported the presence of linoleic, linolenic, and oleic acids in *S. vermiculata* and *S. tetrandra*, underscoring the diversity of fatty acid profiles across the genus. Similarly, Ghorab et al. [64] isolated

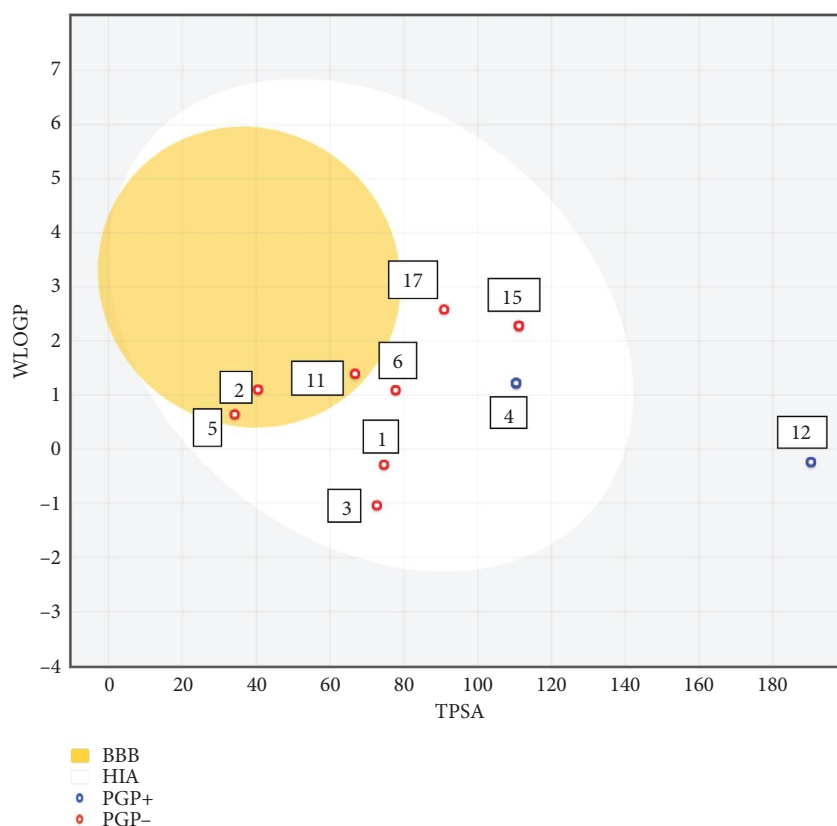


FIGURE 4: BOILED-Egg model of *Salsola kali* identified molecules as evaluated by HPLC-DAD analysis. (1) Fumaric acid; (2) pyrocatechol; (3) theobromine; (4) catechin; (5) methyl-1.4-benzoquinon; (6) caffeic acid; (11) ferulic acid; (12) luteolin 7-O-β-glucoside; (15) fisetin; (17) apigenin.

TABLE 3: AMES toxicity, max. tolerated dose (human), oral rat acute toxicity, hepatotoxicity, and skin sensitization utilizing pkCSM web tool.

Peak	Compound	AMES toxicity	Max. tolerated dose (human) (log mg/kg/day)	Oral rat acute toxicity (LD ₅₀) (mol/kg)	Hepatotoxicity	Skin sensitization
1	Fumaric acid	No	0.69	1.626	No	No
2	Pyrocatechol	No	-0.017	2.14	No	Yes
3	Theobromine	Yes	0.042	2.385	Yes	No
4	Catechin	No	0.438	2.428	No	No
5	Methyl-1.4-benzoquinone	No	1.023	1.816	Yes	No
6	Caffeic acid	No	1.145	2.383	No	No
7	Epicatechin	No	0.438	2.428	No	No
8	Luteolin 7-O-rutinoside	No	0.49	2.515	Yes	No
9	Rutin	No	0.452	2.491	No	No
10	Quercetin 3-O-neohesperidin	No	0.458	2.484	No	No
11	Ferulic acid	No	1.082	2.282	No	No
12	Luteolin 7-O-β-glucoside	No	0.584	2.547	No	No
13	Quercetin 3-O-β-galactoside	No	0.569	2.541	No	No
14	3,5-O-Dicaffeoylquinic acid	No	0.422	2.496	No	No
15	Fisetin	No	0.579	2.465	No	No
16	Luteolin	No	0.499	2.455	No	No
17	Apigenin	No	0.328	2.45	No	No

oleic acid from the aerial parts of *S. tetragona*, reinforcing the importance of unsaturated fatty acids in this species. However, such unsaturated fatty acids were not detected in the hexane extract of *S. kali*, suggesting species-specific differences or solvent-dependent extraction limitations.

The lack of hydroxylated fatty acids, such as hydroxyoctadecenoic acid and trihydroxy derivatives reported by Rasheed et al. [15] in *S. vermiculata* and *S. tetrandra*, also highlights potential variations in fatty acid composition due to species-specific metabolic adaptations or differences in

TABLE 4: Fatty acid composition determined by GC-FID, in *Salsola kali* hexane extract.

Peak	RT	RI	Compound name	Compound class	Concentration (%)
1	24.2	1850	Myristic acid	Saturated fatty acid	0.03
2	28.3	2045	Palmitic acid	Saturated fatty acid	55.17
3	29.4	2100	Heptadecanoic acid	Saturated fatty acid	0.04
4	31.8	2216	3-Hydroxypalmitic acid	Hydroxylated palmitic acid	0.02
5	32.09	2240	Stearic acid	Saturated fatty acid	0.02
6	36.5	2500	Pentacosane	Alkane	0.01
7	39.63	2700	Heptacosane	Alkane	0.11
8	42.66	2900	Nonacosane	Alkane	0.01
9	45.60	3100	Hentriacontane	Alkane	44.58

TABLE 5: Mineral contents of the aerial parts of *Salsola kali* and NIST-CRM 1203 drinking water (mg/kg).

Peak	Mineral contents	mg/g extract	Certified and experimental values of studied metals in NIST-CRM 1203 drinking water (mg/kg) ^a		
			Certified value (mg/kg)	Experimental value ± S.D. (mg/kg) ^b	Recovery value (%)
1	Phosphorus (%)	0.23 ± 0.01	—	—	—
2	Potassium (%)	2.62	—	—	—
3	Calcium (%)	2.27 ± 0.1	99.78 ± 0.50	100.42 ± 0.95	100.64
4	Magnesium (%)	1.3 ± 0.08	99.77 ± 0.50	100.68 ± 1.02	100.23
5	Iron (ppm)	379.82 ± 2.5	200.3 ± 1.0	199.89 ± 2.05	99.94
6	Copper (ppm)	5.28 ± 0.01	2000 ± 10	202.9 ± 0.12	101.45
7	Manganese (ppm)	22.23 ± 0.02	50.17 ± 0.25	50.02 ± 0.75	99.67
8	Zinc (ppm)	33.9 ± 0.03	1000 ± 5	1003.1 ± 7.8	102.59
9	Boron (ppm)	20.67 ± 0.04	—	—	—

Note: Values expressed herein are mean ± SEM of three parallel measurements, *p* < 0.05.

^aTen times dilution of Certified NIST-CRM 1203 drinking water.

^bAverage of triplicate measurements of certified material (*p* < 0.05).

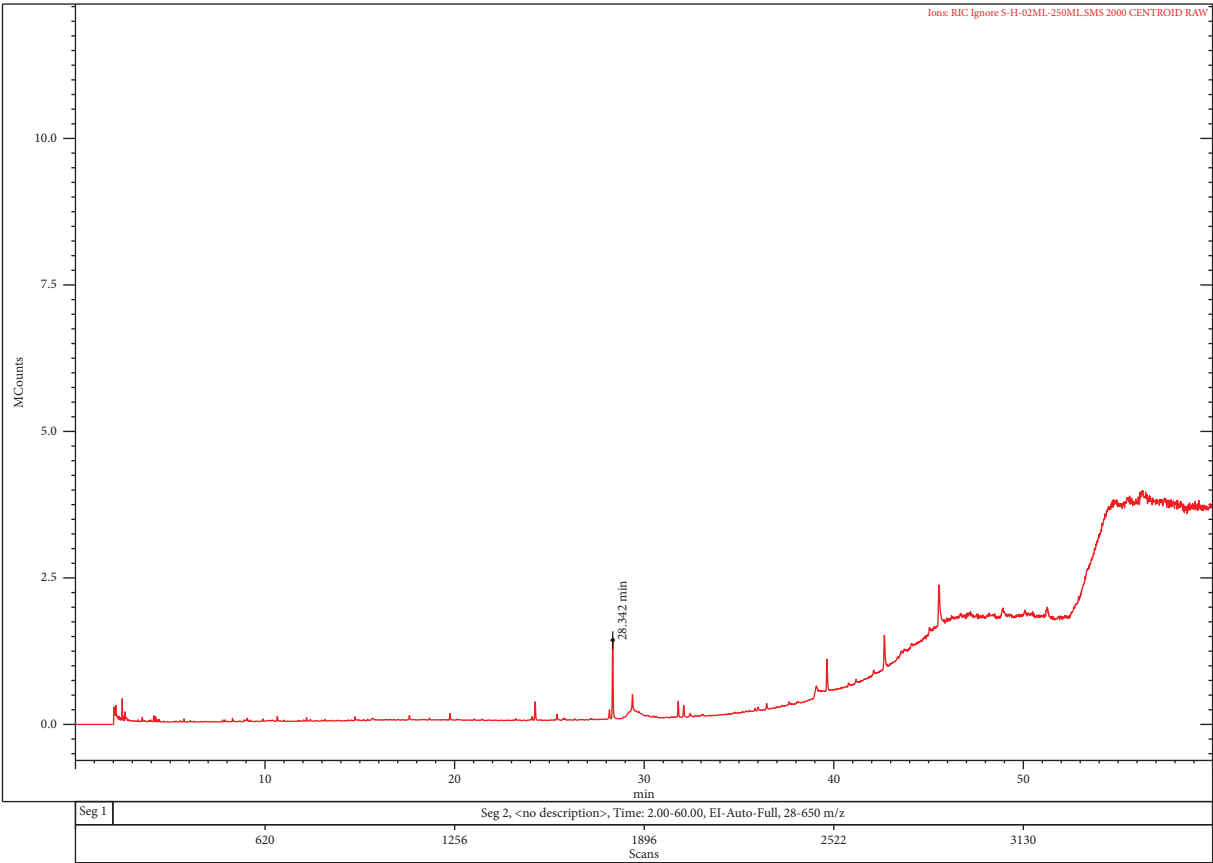


FIGURE 5: GC-FID chromatogram of *Salsola kali*.

extraction techniques. The study by Ghorab et al. [64], which identified 2,3-dihydroxypropylpalmitate from *S. tetragona*, further emphasizes the diversity of fatty acids in the *Salsola* genus. Additionally, the absence of substantial unsaturated fatty acids in *S. kali*, such as linoleic and linolenic acids, may be a reflection of the unusual ecological or evolutionary characteristics that are linked with this species. This could suggest a simplified fatty acid profile predominantly composed of saturated fatty acids, possibly due to the plant's adaptation to specific environmental conditions. These findings complement existing literature by reinforcing the variability in fatty acid composition across *Salsola* species and highlighting the influence of solvent polarity and extraction methods on the detected lipid profile. Further research using polar solvents may provide a more comprehensive understanding of the full range of fatty acids in *S. kali* and their potential biological significance.

3.6. Mineral Analysis. The mineral content analysis of *S. kali* revealed a rich profile of essential macro- and micro-nutrients, with notable concentrations of potassium (2.62%), calcium (2.27%), magnesium (1.3%), and phosphorus (0.23%), indicating its potential for supporting plant metabolism and its nutritional value. Additionally, micro-nutrients like iron (379.82 mg/L), zinc (33.9 mg/L), manganese (22.23 mg/L), copper (5.28 mg/L), and boron (20.67 mg/L) were detected at high levels, highlighting their potential role in enzymatic functions and plant growth. Notably, the current research addresses a critical knowledge gap in the nutritional profile and adaptive strategies of *S. kali* through a comprehensive analysis of its mineral composition (Table 5).

The minerals identified in *S. kali* are essential in various physiological and metabolic processes. Iron, for example, is vital in preventing anemia, supporting hemoglobin and myoglobin synthesis, cellular respiration, DNA synthesis, and the production of iron-dependent enzymes [65]. Calcium contributes to bone and teeth development and the proper functioning of muscles and nerves [66]. Potassium, a key ion for maintaining cellular acid-base and water balance, helps regulate blood pressure, supports bone strength, and is critical for heart and muscle function [44]. Phosphorus is vital for bone mineralization and energy storage, while magnesium plays a significant role in glucose metabolism, diabetes management, bone mineralization, and muscle relaxation [67, 68]. Moreover, trace elements such as manganese, copper, and zinc are essential for cellular and enzymatic functions, including immune regulation, muscle contraction, nerve transmission, and mitochondrial activity [69]. Zinc and copper also enhance antioxidant defenses, contributing to overall cellular health [70, 71]. These minerals and trace elements are essential micronutrients and cofactors in biochemical reactions [72]. The mineral profile of *S. kali* collectively underscores its importance as a valuable source of nutrients with potential health benefits for human beings.

3.7. Antioxidant Activity. The antioxidant capacity of *Salsola kali* methanol and hexane extracts was evaluated using various assays, including DPPH, ABTS, SNP reduction, and reducing power assays (Table 6). The results demonstrate a significant difference in bioactivity depending on the solvent used for extraction. In the DPPH assay, the methanol extract showed moderate antioxidant activity with an IC_{50} value of $90.85 \pm 0.91 \mu\text{g/mL}$, whereas the hexane extract exhibited substantially lower activity ($IC_{50} = 542.59 \pm 2.68 \mu\text{g/mL}$). These findings are consistent with the results of Boulaaba et al. [14] who reported strong DPPH radical scavenging activity for *S. kali* leaf and stem phenolic extracts, with IC_{50} values ranging from 10.67 to 11.67 $\mu\text{g/mL}$, indicating that phenolic content plays a significant role in antioxidant potential [73–75].

Compared to standard antioxidants, methanol and hexane extracts were less effective. BHA ($IC_{50} = 6.14 \pm 0.41 \mu\text{g/mL}$) and BHT ($IC_{50} = 12.99 \pm 0.41 \mu\text{g/mL}$) significantly outperformed both extracts, highlighting the higher potency of synthetic antioxidants. This observation aligns with El Basossy et al. [23] findings, who reported stronger DPPH scavenging activity in ethyl acetate extracts compared to methanolic extracts of *S. kali* ($IC_{50} = 41.52 \mu\text{g/mL}$). Based on these differences, it appears that the polarity of the solvent has a major impact on the extraction efficiency of bioactive molecules that are responsible for antioxidant activity.

In the ABTS assay, the methanol extract exhibited more substantial antioxidant capacity ($IC_{50} = 26.76 \pm 0.47 \mu\text{g/mL}$) compared to the hexane extract ($IC_{50} = 84.20 \pm 1.45 \mu\text{g/mL}$). This finding aligns with previous reports from Mohamed et al. [54] who demonstrated the importance of solvent type in enhancing ABTS radical scavenging efficiency, as observed in aqueous-ethanolic extracts of *S. cyclophylla*. It is probable that the ability of the methanol extract to solubilize phenolic and flavonoid components more efficiently than hexane is the reason for its greater antioxidant capability in both the DPPH and ABTS experiments.

Interestingly, a contrasting pattern was observed in the SNP reduction assay. Here, the hexane extract showed higher antioxidant activity ($A_{0.5} = 26.51 \mu\text{g/mL}$) than the methanol extract ($A_{0.5} = 35.00 \mu\text{g/mL}$). This contrasts with the trends observed in DPPH and ABTS assays, suggesting that hexane extracts might contain lipophilic compounds with a stronger affinity for silver ion reduction, a finding consistent with the work of Boulaaba et al. [14] who highlighted variations in antioxidant activity depending on the organ and solvent used.

In the reducing power assay, the methanol extract showed moderate activity ($A_{0.5} = 57.10 \pm 0.75 \mu\text{g/mL}$). On the other hand, the hexane extract had a level of activity that was substantially lower ($A_{0.5} > 200 \mu\text{g/mL}$). These results agree with Boulaaba et al. [14] who reported significant reducing power for phenolic extracts of *S. kali*, although still less potent than ascorbic acid ($A_{0.5} = 6.77 \pm 1.15 \mu\text{g/mL}$). Similarly, findings by Aytar et al. [20] on *S. baryosma* ethanol extracts reported strong reducing power, further supporting the importance of solvent selection in maximizing antioxidant extraction.

TABLE 6: Antioxidant activities (IC_{50} and $A_{0.5}$ values) of *Salsola kali* methanol and hexane extracts.

	DPPH assay IC_{50} ($\mu\text{g/mL}$)	ABTS assay IC_{50} ($\mu\text{g/mL}$)	SNP assay $A_{0.5}$ ($\mu\text{g/mL}$)	Reducing power assay $A_{0.5}$ ($\mu\text{g/mL}$)
Methanol extract	90.85 \pm 0.91	26.76 \pm 0.47	35.00 \pm 0.31	57.10 \pm 0.75
Hexane extract	542.59 \pm 2.68	84.20 \pm 1.45	26.51 \pm 0.23	> 200
BHA	6.14 \pm 0.41	1.29 \pm 0.30	73.47 \pm 0.88	nd
BHT	12.99 \pm 0.41	1.81 \pm 0.10	nd	nd
α -Tocopherol	13.02 \pm 5.17	nd	nd	34.93 \pm 2.38
Ascorbic acid	nd	nd	> 200	6.77 \pm 1.15
Trolox	nd	nd	34.17 \pm 1.23	nd

Note: Values expressed herein are mean \pm SEM of three parallel measurements, $p < 0.05$; BHA: butylated hydroxyanisole. Abbreviation: nd = not detected.

TABLE 7: Anticholinesterase and antidiabetic activities (IC_{50} values) of *Salsola kali* methanol and hexane extracts.

Extracts & compounds	Anticholinesterase activity IC_{50} ($\mu\text{g/mL}$)		Antidiabetic inhibitory activities IC_{50} ($\mu\text{g/mL}$)	
	AChE	BChE	α -Amylase	α -Glucosidase
Concentrations tested ($\mu\text{g/mL}$)	25–200	25–200	50–400	25–200
Methanolic extract	> 200	242.00 \pm 1.52	315.70 \pm 2.00	NA
Hexane extract	NA	536.62 \pm 0.83	437.03 \pm 1.02	47.86 \pm 2.83
Galantamine ^a	4.44 \pm 1.57	30.79 \pm 0.13	NT	NT
Acarbose ^a	NT	NT	36.74 \pm 4.50	22.28 \pm 2.03

Note: Values expressed herein are mean \pm SEM of three parallel measurements. $p < 0.05$.

Abbreviations: NA = not active; NT = not tested.

^aReference compounds.

Also, when contextualized with findings from other *Salsola* species, the methanol extract of *S. kali* demonstrated moderate antioxidant activity. Still, it remained less effective than extracts from *S. baryosma* and *S. cyclophylla* [54]. Djerdjane et al. [75] highlight that different species of *Salsola* may exhibit varying antioxidant potentials due to differences in phenolic content and phytochemical composition. The results of this study underscore the superior performance of methanol extracts over hexane extracts in most assays, likely due to the higher solubility of phenolic compounds in methanol. However, the higher activity of standard antioxidants like BHA and ascorbic acid suggests that future research should focus on optimizing extraction methods to enhance the bioactivity of *S. kali* extracts by concentrating the phenolic and flavonoid content.

3.8. Enzyme Inhibitory Capacity. The enzyme inhibitory potential of *Salsola kali* methanol extract was evaluated for its ability to inhibit key enzymes associated with metabolic disorders, particularly BChE, α -amylase, and α -glucosidase (Table 7). The methanol extract demonstrated moderate inhibitory activity against BChE, aligning with previous findings on *Salsola* species, which suggest the neuroprotective potential of traditional plant extracts. However, data regarding AChE inhibition were below 200 $\mu\text{g/mL}$ for the methanolic extract, which was inactive in this study, limiting a comprehensive assessment of cholinesterase inhibitory activity.

In terms of antidiabetic potential, the methanol extract displayed notable α -glucosidase inhibitory activity, suggesting its potential application for managing postprandial hyperglycemia. Although the α -amylase inhibitory activity was comparatively lower, these findings align with previous studies highlighting the potential of *Salsola* species for managing carbohydrate metabolism. Tundis et al. [17] previously reported α -amylase inhibition in various *Salsola* fractions, with the ethyl acetate extract of *S. kali* showing the highest potency ($IC_{50} = 0.022 \text{ mg/mL}$).

In contrast to previous reports, the methanol extract of *S. kali* showed no measurable α -glucosidase inhibitory activity ($IC_{50} = \text{NA}$ within 25–200 $\mu\text{g/mL}$). This discrepancy may be attributed to variations in solvent polarity, plant chemotype, or experimental design.

Comparative studies with related species, such as *S. baryosma* and *S. vermiculata*, suggest that these species exhibit stronger α -amylase and α -glucosidase inhibitory activities, as reported by Djerdjane et al. [75]. However, since K_i values were not determined in the present study, a direct comparison with other research is impossible. Despite this limitation, the presence of α -glucosidase inhibitory activity in other extracts of *S. kali* supports the possibility that additional bioactive compounds may contribute to its antidiabetic potential.

Further support for the potential of *S. kali* comes from studies on other *Salsola* species. Jin et al. [12] reported that *S. collina* contains N-acetyltryptophan, which exhibited 44% inhibition of α -amylase activity. Although similar

compounds were not isolated in this study, phenolic compounds like pyrocatechol and epicatechin in *S. kali* could explain its inhibitory effect on α -glucosidase. Additionally, Iannuzzi et al. [76] demonstrated that quercetin derivatives from *S. soda* inhibited aldose reductase enzymes, suggesting the broader antidiabetic potential of the *Salsola* genus.

4. Conclusions

This study highlights the significant bioactive potential of *Salsola kali*, emphasizing its rich phytochemical composition, antioxidant properties, and enzyme inhibitory activities. The methanolic extract, enriched with phenolic compounds like pyrocatechol, epicatechin, and chlorogenic acid, exhibited strong antioxidant activity in DPPH and ABTS assays. Conversely, the hexane extract demonstrated potent α -glucosidase inhibition, suggesting its potential for managing postprandial hyperglycemia. ADME analysis is a cornerstone of modern drug development and toxicology. It gives critical insights into how a molecule interacts with the body, which is crucial for determining its safety, efficacy, and potential as a therapeutic agent. In this report, the detailed analysis of ADME indicated favorable pharmacokinetic profiles for key constituents, with 11 compounds adhering to Lipinski's rule of five and 6 violating the rule. Moreover, *Salsola kali* has low toxicity profiles indicating that most of compounds are nonmutagenic and non-hepatotoxic, making them potentially safe for further pharmacological and effective use in traditional or modern medicine. Additionally, the plant's mineral profile, rich in essential nutrients such as potassium, calcium, and iron, further supports its nutritional value. These findings position *S. kali* as a promising natural resource for developing nutraceuticals or therapeutic agents targeting oxidative stress, neurodegenerative disorders, and diabetes. Future research should focus on in vivo validation, isolation of bioactive principles, and optimization of extraction techniques to enhance bioactivity. Exploring its environmental applications, such as phytoremediation, could further enhance the value of this halophytic species.

Data Availability Statement

The data will be available upon request to the authors.

Ethics Statement

The conducted research is not related to either human or animal use.

Conflicts of Interest

The authors declare no conflicts of interest.

Author Contributions

Conceptualization: H.B. and M.Ö.; data curation: G.G.S. and F.B.; formal analysis: M.Ö.; funding acquisition: H.B. and F.B.; investigation: H.R. and G.G.S.; methodology: M.Ö. and H.B.; project administration: K.R.; resources: K.R. and M.Ö.;

software: M.Ö.; supervision: H.B. and S.G.; validation: H.B.; visualization: M.Ö.; writing—original draft: H.R. and H.B.; and writing—review and editing: B.A., S.R.C., E.W., and S.G. All authors reviewed the manuscript.

Funding

This work was supported and funded by the Deanship of Scientific Research at Imam Mohammad Ibn Saud Islamic University (IMSIU) (grant number IMSIU-DDRSP2501).

References

- [1] M. H. ElNaggar, W. M. Eldehna, M. A. Abourehab, and F. M. Abdel Bar, "The Old World *Salsola* as a Source of Valuable Secondary Metabolites Endowed with Diverse Pharmacological Activities: a Review," *Journal of Enzyme Inhibition and Medicinal Chemistry* 37, no. 1 (2022): 2036–2062, <https://doi.org/10.1080/14756366.2022.2102005>.
- [2] V. Altay and M. Ozturk, "The Genera *Salsola* and *Suaeda* (Amaranthaceae) and Their Value as Fodder," *Handbook of Halophytes* (2020): 1–12, https://doi.org/10.1007/978-3-030-17854-3_97-1.
- [3] K. Idzikowska, "Morphological and Anatomical Structure of Generative Organs of *Salsola kali* Ssp. *Ruthenica* [Iljin] Soo at the SEM Level," *Acta Societatis Botanicorum Poloniae* 74 (2005): 99–109.
- [4] B. S. Chauhan, A. Tanveer, G. Rasool, Z. Hanif, and H. H. Ali, "Genus *Salsola*: Its Benefits, Uses, Environmental Perspectives and Future aspects—A Review," *J. Rangel. Sci.* 8 (2018): 315–328.
- [5] R. Klopfer and A. Van Wyk, "The Genus *Salsola* (Chenopodiaceae) in Southern Africa: Systematic Significance of Leaf Anatomy," *South African Journal of Botany* 67, no. 4 (2001): 540–551, [https://doi.org/10.1016/s0254-6299\(15\)31186-8](https://doi.org/10.1016/s0254-6299(15)31186-8).
- [6] K. N. Toderich, E. V. Shuyskaya, M. Ozturk, A. Juylova, and L. Gismatulina, "Pollen Morphology of Some Asiatic Species of Genus *Salsola* (Chenopodiaceae) and Its Taxonomic Relationships," *Pakistan Journal of Botany* 42 (2010): 155–174.
- [7] H. H. Sonyan and A. M. Hayrapetyan, "Statistical Analysis of the Basic Morphological Characteristics of Pollen Within the Limits of Genus *Salsola* L. Sensus Lato in South Transcaucasia," *ЕСТЕСТВЕННЫЕ НАУКИ* 1 (2021): 36.
- [8] S. Ahmed, M. Ashraf, A. Jabbar, et al., "Pharmacological Screening of *Salsola Baryosma*," *Journal of the Chemical Society of Pakistan* 28, no. 1 (2006): 82.
- [9] A. Beyaoui, A. Chaari, H. Ghouila, M. Ali Hamza, and H. Ben Jannet, "New Antioxidant Bibenzyl Derivative and Isoflavonoid from the Tunisian *Salsola tetrandra* Folsk," *Natural Product Research* 26, no. 3 (2012): 235–242, <https://doi.org/10.1080/14786419.2010.536950>.
- [10] A. Sokolowska-Krzaczek, K. Skalicka-Wozniak, and K. Czubkowska, "Variation of Phenolic Acids from Herb and Roots of *Salsola kali* L.," *Acta Societatis Botanicorum Poloniae* 78, no. 3 (2009): 197–201.
- [11] M. Topal, "Secondary Metabolites of Ethanol Extracts of *Pinus sylvestris* Cones from Eastern Anatolia and Their Antioxidant, Cholinesterase and α -glucosidase Activities," *Records of Natural Products* 14, no. 2 (2019): 129–138, <https://doi.org/10.25135/rnp.155.19.06.1326>.
- [12] Y. S. Jin, J. L. Du, Y. Yang, et al., "Chemical and Biologically Active Constituents of *Salsola Collina*," *Chemistry of Natural*

- Compounds* 47, no. 2 (2011): 257–260, <https://doi.org/10.1007/s10600-011-9896-2>.
- [13] S. S. Murshid, D. Atoum, D. R. Abou-Hussein, et al., “Genus Salsola: Chemistry, Biological Activities and Future prospective—A Review,” *Plants* 11, no. 6 (2022): 714, <https://doi.org/10.3390/plants11060714>.
 - [14] M. Boulaaba, F. Medini, H. Hajlaoui, et al., “Biological Activities and Phytochemical Analysis of Phenolic Extracts from *Salsola kali* L. Role of Endogenous Factors in the Selection of the Best Plant Extracts,” *South African Journal of Botany* 123 (2019): 193–199, <https://doi.org/10.1016/j.sajb.2019.03.003>.
 - [15] D. M. Rasheed, S. M. El Zalabani, M. A. Koheil, H. M. El-Hefnawy, and M. A. Farag, “Metabolite Profiling Driven Analysis of *Salsola* Species and Their Anti-acetylcholinesterase Potential,” *Natural Product Research* 27, no. 24 (2013): 2320–2327, <https://doi.org/10.1080/14786419.2013.832676>.
 - [16] M. H. Oueslati, H. B. Jannet, Z. Mighri, J. Chriaa, and P. M. Abreu, “Phytochemical Components from *Salsola tetrandra*,” *Journal of Natural Products* 69 (2006): 1366–1369.
 - [17] R. Tundis, M. R. Loizzo, G. A. Statti, and F. Menichini, “Inhibitory Effects on the Digestive Enzyme α -amylase of Three *Salsola* Species (Chenopodiaceae) in Vitro,” *Pharmazie* 62, no. 6 (2007): 473–475.
 - [18] P. Swart, A. C. Swart, A. Louw, and K. J. van der Merwe, “Biological Activities of the Shrub *Salsola tuberculatifomis* Botsch.: Contraceptive or Stress Alleviator?” *BioEssays* 25, no. 6 (2003): 612–619, <https://doi.org/10.1002/bies.10285>.
 - [19] M. Chaieb and M. Boukhris, “Flore Succinte Et Illustrée Des Zones Arides Et Sahariennes De Tunisie. L’Or Du Temps” (1998).
 - [20] E. C. Aytar, B. Aydın, E. I. Torunoğlu, and A. Durmaz, “Antimicrobial Activity and Molecular Docking Analysis of *Salsola Kali*: Investigating Potent Biological Interactions and Chemical Composition,” *Journal of Herbal Medicine* 48 (2024): 100942, <https://doi.org/10.1016/j.hermed.2024.100942>.
 - [21] S. Hasan, R. Sobhian, and F. Herard, “Biology, Impact and Preliminary host-specificity Testing of the Rust Fungus, *Uromyces salsolae*, a Potential Biological Control Agent for *Salsola kali* in the USA,” *Biocontrol Science and Technology* 11, no. 6 (2001): 677–689, <https://doi.org/10.1080/09583150120093040>.
 - [22] A. Hameed, N. Ghani, T. A. Mughal, M. Abbas, A. Abrar, and H. Javed, “Pharmacognostical Evaluation and Physiochemical Analysis of *Salsola kali* as Medicinal Plant,” *Microscopy Research and Technique* 86, no. 10 (2023): 1322–1332, <https://doi.org/10.1002/jemt.24316>.
 - [23] T. A. I. El-Bassossy, A. A. Abdelgawad, and D. elazab, “Pharmacological Investigations and Chemical Constituents of *Salsola kali* Aerial Parts,” *Egyptian Journal of Chemistry* 0, no. 0 (2023): 0–2044, <https://doi.org/10.21608/ejchem.2023.232570.8526>.
 - [24] V. Nath and P. K. Khatri, “Traditional Knowledge on ethno-medicinal Uses Prevailing in Tribal Pockets of Chhindwara and Betul Districts, Madhya Pradesh, India,” *African Journal of Pharmacy and Pharmacology* 4, no. 9 (2010): 662–670.
 - [25] R. Tundis, F. Menichini, F. Conforti, et al., “A Potential Role of Alkaloid Extracts from *Salsola* Species (Chenopodiaceae) in the Treatment of Alzheimer’s Disease,” *Journal of Enzyme Inhibition and Medicinal Chemistry* 24, no. 3 (2009): 818–824, <https://doi.org/10.1080/14756360802399662>.
 - [26] K. Ben Rejeb, T. Ghnaya, H. Zaier, et al., “Evaluation of the Cd²⁺ Phytoextraction Potential in the Xerohalophyte *Salsola kali* L. and the Impact of EDTA on This Process,” *Ecological Engineering* 60 (2013): 309–315, <https://doi.org/10.1016/j.ecoleng.2013.07.026>.
 - [27] E. Neagu, G. Paun, C. Albu, and G. L. Radu, “Valorization of Bioactive Compounds from Lingonberry Pomace and Grape Pomace with Antidiabetic Potential,” *Molecules* 29, no. 22 (2024): 5443, <https://doi.org/10.3390/molecules29225443>.
 - [28] Z. Lisiewska, W. Kmiecik, and A. Korus, “Content of Vitamin C, Carotenoids, Chlorophylls and Polyphenols in Green Parts of Dill (*Anethum graveolens* L.) Depending on Plant Height,” *Journal of Food Composition and Analysis* 19, no. 2–3 (2006): 134–140, <https://doi.org/10.1016/j.jfca.2005.04.009>.
 - [29] M. Ozyurek, N. Gungor, S. Baki, K. Guclu, and R. Apak, “Development of a Silver Nanoparticle-based Method for the Antioxidant Capacity Measurement of Polyphenols,” *Analytical Chemistry* 84, no. 18 (2012): 8052–8059, <https://doi.org/10.1021/ac301925b>.
 - [30] I. Jallali, W. Megdiche, B. M’ Hamdi, et al., *Acta Physiologiae Plantarum* 34 (2012): 1451.
 - [31] Powo (Plants of the World Online), “The International Plant Names Index and World Checklist of Vascular Plants 2025,” (2025), <https://powo.science.kew.org/taxon/urn:lsid:ipni.org:names:303401-2>.
 - [32] P. Quezel and S. Santa, “New Flora of Algeria and Southern Desert Regions” (1962).
 - [33] D. J. Mabberley, *The Plant Book: A Portable Dictionary of the Vascular Plants* (Cambridge University Press, 1997).
 - [34] A. Mokhtar, T. Souhila, B. Nacéra, et al., “In Vitro Antibacterial, Antioxidant, Anticholinesterase, and Antidiabetic Activities and Chemical Composition of *Salvia balansae*,” *Molecules* 28, no. 23 (2023): 7801, <https://doi.org/10.3390/molecules28237801>.
 - [35] A. Ertas, M. Firat, I. Yener, et al., “Phytochemical Fingerprints and Bioactivities of Ripe Disseminules (fruit-seeds) of Seventeen *Gundelia* (Kenger-Kereng Dikeni) Species from Anatolia with Chemometric Approach,” *Chemistry and Biodiversity* 18, no. 8 (2021): e2100207, <https://doi.org/10.1002/cbdv.202100207>.
 - [36] B. Aouzal, F. Oudjane, L. Bourouh, et al., “Elucidating the Dual agro-biochemical Roles of *Dittrichia viscosa* Methanolic and Ethanolic Extracts: Biostimulant-Driven Germination, Crop Enhancement, and Antioxidant Synergy,” *Ciencia E Agrotecnologia* 49, no. 1 (2025): e006925–14, <https://doi.org/10.1590/1413-7054202549006925>.
 - [37] Ö. Tokul-Ölmez, B. Sahin, C. Çakır, and M. Ozturk, “Rapid and Easy Method for Simultaneous Measurement of Widespread 27 Compounds in Natural Products and Foods,” *Journal of Chemical Metrology* 14, no. 1 (2020): 1–11, <https://doi.org/10.25135/jcm.38.20.03.1589>.
 - [38] D. K. Lee, J. In, and S. Lee, “Standard Deviation and Standard Error of the Mean,” *Korean Journal of Anesthesiology* 68, no. 3 (2015): 220–223, <https://doi.org/10.4097/kjae.2015.68.3.220>.
 - [39] A. Daina, O. Michielin, and V. Zoete, “Swissadme: a Free Web Tool to Evaluate Pharmacokinetics, drug-likeness and Medicinal Chemistry Friendliness of Small Molecules,” *Scientific Reports* 7, no. 1 (2017): 42717, <https://doi.org/10.1038/srep42717>.
 - [40] T. S. Maliehe, P. H. Tsilo, and J. S. Shandu, “Computational Evaluation of ADMET Properties and Bioactive Score of Compounds from *Encephalartos ferox*,” *Pharmacognosy Journal* 12, no. 6 (2020): 1357–1362, <https://doi.org/10.5530/pj.2020.12.187>.
 - [41] D. E. Pires, T. L. Blundell, and D. B. Ascher, “PkcsM: Predicting small-molecule Pharmacokinetic and Toxicity Properties Using Graphbased Signatures,” *Journal of Medicinal*

- Chemistry* 58, no. 9 (2015): 4066–4072, <https://doi.org/10.1021/acs.jmedchem.5b00104>.
- [42] D. Çam, C. Çakır, A. H. Karaman, et al., “Characterization of the Cytotoxic Compounds of *Lactarius Salmonicolor* R. Heim and Leclair by Gas chromatography-mass Spectrometry and Chemometrics,” *Analytical Letters* (2025).
 - [43] N. Cicero, T. Gervasi, A. Durazzo, et al., “Mineral and Microbiological Analysis of Spices and Aromatic Herbs,” *Foods* 11, no. 4 (2022): 548, <https://doi.org/10.3390/foods11040548>.
 - [44] G. Tel-Cayan, Z. Ullah, M. Ozturk, M. Yabanlı, F. Aydın, and M. E. Duru, “Heavy Metals, Trace and Major Elements in 16 Wild Mushroom Species Determined by ICP-MS,” *Atomic Spectroscopy* 39, no. 01 (2018): 29–37, <https://doi.org/10.46770/as.2018.01.004>.
 - [45] M. S. Blois, “Antioxidant Determinations by the Use of a Stable Free Radical,” *Nature* 181, no. 4617 (1958): 1199–1200, <https://doi.org/10.1038/1811199a0>.
 - [46] B. Aouzal, *Moderation of the Toxic Effects of the Fungicide Tebuconazole by the Extract of Ruta Montana in Wistar Rats* (University of Skikda, 2025).
 - [47] R. Re, N. Pellegrini, A. Proteggente, A. Pannala, M. Yang, and C. Rice-Evans, “Antioxidant Activity Applying an Improved ABTS Radical Cation Decolorization Assay,” *Free Radical Biology and Medicine* 26, no. 9-10 (1999): 1231–1237, [https://doi.org/10.1016/s0891-5849\(98\)00315-3](https://doi.org/10.1016/s0891-5849(98)00315-3).
 - [48] M. Oyaizu, “Studies on Products of Browning Reactions: Antioxidative Activities of Browning Reaction Prepared from Glucosamine,” *The Japanese Journal of Nutrition and Dietetics* 44, no. 6 (1986): 307–315, <https://doi.org/10.5264/eiyogakuzashi.44.307>.
 - [49] G. L. Ellman, K. D. Courtney, V. Andres, and R. M. Featherstone, “A New and Rapid Colorimetric Determination of Acetylcholinesterase Activity,” *Biochemical Pharmacology* 7, no. 2 (1961): 88–95, [https://doi.org/10.1016/0006-2952\(61\)90145-9](https://doi.org/10.1016/0006-2952(61)90145-9).
 - [50] N. V. Quan, T. D. Xuan, H. D. Tran, A. Ahmad, T. D. Khanh, and T. D. Dat, “Contribution of Momilactones A and B to Diabetes Inhibitory Potential of Rice Bran: Evidence from in Vitro Assays,” *Saudi Pharmaceutical Journal* 27, no. 5 (2019): 643–649, <https://doi.org/10.1016/j.jsps.2019.03.006>.
 - [51] J. S. Kim, Y. S. Kwon, W. J. Chun, et al., “*Rhus verniciflua* Stokes Flavonoid Extracts Have Anti-oxidant, Anti-microbial and α -glucosidase Inhibitory Effect,” *Food Chemistry* 120, no. 2 (2010): 539–543, <https://doi.org/10.1016/j.foodchem.2009.10.051>.
 - [52] I. Ounissi, S. Slimani, J. Bounaas, C. Bensouici, B. Aouzal, and A. Bouacha, “Phytochemical Profile by LC-MS/MS, Total Phenolic Content and Antioxidant Properties of *Erodium guttatum* from Algeria,” *Global NEST Journal* 26, no. 10 (2024): 1–10, <https://doi.org/10.30955/gnj.06464>.
 - [53] N. G. Shehab, E. Abu-Gharbieh, and F. A. Bayoumi, “Impact of Phenolic Composition on Hepatoprotective and Antioxidant Effects of Four Desert Medicinal Plants,” *BMC Complementary and Alternative Medicine* 15 (2015): 401–412, <https://doi.org/10.1186/s12906-015-0919-6>.
 - [54] H. A. Mohammed, M. S. Al-Omar, S. A. Mohammed, et al., “Phytochemical Analysis, Pharmacological and Safety Evaluations of Halophytic Plant, *Salsola cyclophylla*,” *Molecules* 26, no. 8 (2021): 2384, <https://doi.org/10.3390/molecules26082384>.
 - [55] I. Laib, D. Eddine Laib, D. Semouma, et al., “Optimization of Extraction and Study of the in Vitro Static Simulation of INFOGEST Gastrointestinal Digestion and in Vitro Colonic Fermentation on the Phenolic Compounds of Dandelion and Their Antioxidant Activities,” *Journal of Food Measurement and Characterization* 17, no. 6 (2023): 5660–5682, <https://doi.org/10.1007/s11694-023-02083-4>.
 - [56] B. Aouzal, S. Slimani, F. Kamah, I. Ounissi, A. Bouacha, and S. Elmokli, “LC-MS/MS Phytochemical Analysis of *Ruta Montana* and the Hepatic Preventive Effects in Male Rats Exposed to Tebuconazole,” *Global NEST Journal* 26, no. 10 (2024): <https://doi.org/10.30955/gnj.06877>.
 - [57] C. A. Lipinski, F. Lombardo, B. W. Dominy, and P. J. Feeney, “Experimental and Computational Approaches to Estimate Solubility and Permeability in Drug Discovery and Development Settings,” *Advanced Drug Delivery Reviews* 46, no. 1–3 (2001): 3–26, [https://doi.org/10.1016/S0169-409X\(00\)00129-0](https://doi.org/10.1016/S0169-409X(00)00129-0).
 - [58] I. Muegge, S. L. Heald, and D. Brittelli, “Simple Selection Criteria for Drug-like Chemical Matter,” *Journal of Medicinal Chemistry* 44, no. 12 (2001): 1841–1846, <https://doi.org/10.1021/jm015507e>.
 - [59] J. A. Arnott and S. L. Planey, “The Influence of Lipophilicity in Drug Discovery and Design,” *Expert Opinion on Drug Discovery* 7, no. 10 (2012): 863–875, <https://doi.org/10.1517/17460441.2012.714363>.
 - [60] K. Hchicha, M. Korb, R. Badraoui, and H. Naili, “A Novel sulfate-bridged Binuclear Copper (II) Complex: Structure, Optical, ADMET and in Vivo Approach in a Murine Model of Bone Metastasis,” *New Journal of Chemistry* 45, no. 31 (2021): 13775–13784, <https://doi.org/10.1039/d1nj02388h>.
 - [61] S. Jebahi, G. Ben Salah, S. Jarray, et al., “Chitosan-Based Gastric Dressing Materials Loaded with Pomegranate Peel as Bioactive Agents: Pharmacokinetics and Effects on Experimentally Induced Gastric Ulcers in Rabbits,” *Metabolites* 12, no. 12 (2022): 1158, <https://doi.org/10.3390/metabo12121158>.
 - [62] I. Bédoui, H. B. Nasr, K. Ksouda, et al., “Phytochemical Composition, Bioavailability and Pharmacokinetics of *Scorzonera undulata* Methanolic Extracts: Antioxidant, Anticancer, and Apoptotic Effects on MCF7 Cells,” *Pharmacognosy Magazine* 20, no. 1 (2024): 218–229, <https://doi.org/10.1177/09731296231207231>.
 - [63] E. H. Kerns and L. Di, “Pharmaceutical Profiling in Drug Discovery,” *Drug Discovery Today* 8, no. 7 (2003): 316–323, [https://doi.org/10.1016/s1359-6446\(03\)02649-7](https://doi.org/10.1016/s1359-6446(03)02649-7).
 - [64] H. Ghorab, A. Khettaf, M. Lehbili, et al., “A New Cardenolide and Other Compounds from *Salsola tetragona*,” *Natural Product Communications* 12, no. 1 (2017): 1934578X1701200102, <https://doi.org/10.1177/1934578X1701200102>.
 - [65] N. Abbaspour, R. Hurrell, and R. Kelishadi, “Review on Iron and Its Importance for Human Health,” *Journal of Research in Medical Sciences: The Official Journal of Isfahan University of Medical Sciences* 19, no. 2 (2014): 164–174.
 - [66] J. A. Beto, “The Role of Calcium in Human Aging,” *Clinical nutrition research* 4, no. 1 (2015): 1–8, <https://doi.org/10.7762/cnr.2015.4.1.1>.
 - [67] G. Tel, M. Öztürk, M. E. Duru, B. Doğan, and M. Harmandar, “Fatty Acid Composition, Antioxidant, Anticholinesterase and Tyrosinase Inhibitory Activities of Four *Serratula* Species from Anatolia,” *Records of Natural Products* 7, no. 2 (2013).
 - [68] A. M. Al Alawi, S. W. Majoni, and H. Falhammar, “Magnesium and Human Health: Perspectives and Research Directions,” *International journal of endocrinology* 2018, no. 1 (2018): 1–17, <https://doi.org/10.1155/2018/9041694>.
 - [69] M. H. Siddiqui and M. H. Al-Whaibi, “Role of nano-SiO₂ in Germination of Tomato (*Lycopersicon Esculentum* Seeds Mill.),” *Saudi Journal of Biological Sciences* 21, no. 1 (2014): 13–17, <https://doi.org/10.1016/j.sjbs.2013.04.005>.

- [70] J. W. Spears and W. P. Weiss, "Role of Antioxidants and Trace Elements in Health and Immunity of Transition Dairy Cows," *The Veterinary Journal* 176, no. 1 (2008): 70–76, <https://doi.org/10.1016/j.tvjl.2007.12.015>.
- [71] P. S. Negi, "Plant Extracts for the Control of Bacterial Growth: Efficacy, Stability and Safety Issues for Food Application," *International Journal of Food Microbiology* 156, no. 1 (2012): 7–17, <https://doi.org/10.1016/j.ijfoodmicro.2012.03.006>.
- [72] J. R. Calabrese, A. D. Gullledge, K. Hahn, et al., "Autoimmune Thyroiditis in manic-depressive Patients Treated with Lithium," *American Journal of Psychiatry* 142, no. 11 (1985): 1318–1321, <https://doi.org/10.1176/ajp.142.11.1318>.
- [73] N. Messaoudi, I. Haoueme, B. Aouzal, M. M. Djamel, Z. Hadjer, and H. Bendif, "Phytochemical Screening, Polyphenols Content and Antioxidant Activities of Some Selected Medicinal Plants Growing in Algeria," *Natural Resources and Sustainable Development* 15, no. 1 (2025): 189–202, <https://doi.org/10.31924/nrsd.v15i1.185>.
- [74] I. Khacheba, A. Djeridane, A. Kameli, and M. Yousfi, "The Inhibitory Effect of Some Algerian Plants Phenolics Extracts on the α -glucosidase and α -amylase Activities and Their Antioxidant Activities," *Current Enzyme Inhibition* 10, no. 1 (2013): 59–68, <https://doi.org/10.2174/15734080113099990001>.
- [75] A. Djeridane, A. Hamdi, W. Bensania, K. Cheifa, I. Lakhdari, and M. Yousfi, "The in Vitro Evaluation of Antioxidative Activity, α -glucosidase and α -amylase Enzyme Inhibitory of Natural Phenolic Extracts," *Diabetes & Metabolic Syndrome: Clinical Research & Reviews* 9, no. 4 (2015): 324–331, <https://doi.org/10.1016/j.dsx.2013.10.007>.
- [76] A. M. Iannuzzi, R. Moschini, M. De Leo, et al., "Chemical Profile and Nutraceutical Features of *Salsola soda* (Agretti): Anti-Inflammatory and Antidiabetic Potential of Its Flavonoids," *Food Bioscience* 37 (2020): 100713, <https://doi.org/10.1016/j.fbio.2020.100713>.